Protein-Cofactor Interactions in Bacterial Reaction Centers from *Rhodobacter sphaeroides* R-26: I. Identification of the ENDOR Lines Associated with the Hydrogen Bonds to the Primary Quinone $Q_A^{\cdot -}$

M. Flores,*† R. Isaacson,* E. Abresch,* R. Calvo,*‡ W. Lubitz,† and G. Feher*

*Department of Physics, University of California at San Diego, La Jolla, California; †Max-Planck Institut für Bioanorganische Chemie, Mülheim an der Ruhr, Germany; and ‡Departamento de Física, Facultad de Bioquímica y Ciencias Biológicas and INTEC, Universidad Nacional del Litoral and CONICET, Santa Fe, Argentina

ABSTRACT Hydrogen bonds are important in determining the structure and function of biomolecules. Of particular interest are hydrogen bonds to quinones, which play an important role in the bioenergetics of respiration and photosynthesis. In this work we investigated the hydrogen bonds to the two carbonyl oxygens of the semiquinone $Q_A^{\cdot -}$ in the well-characterized reaction center from the photosynthetic bacterium *Rhodobacter sphaeroides* R-26. We used electron paramagnetic resonance and electron nuclear double resonance techniques at 35 GHz at a temperature of 80 K. The goal of this study was to identify and assign sets of ^{1}H-ENDOR lines to protons hydrogen bonded to each of the two oxygens. This was accomplished by preferentially exchanging the hydrogen bond on one of the oxygens with deuterium while concomitantly monitoring the changes in the amplitudes of the ^{1}H-ENDOR lines. The preferential deuteration of one of the oxygens was made possible by the different $^1H \rightarrow {}^2H$ exchange times of the protons bonded to the two oxygens. The assignment of the ^{1}H-ENDOR lines sets the stage for the determination of the geometries of the H-bonds by a detailed field selection ENDOR study to be presented in a future article.

INTRODUCTION

Quinones play an important role as cofactors in many proteins (1,2). Their biological function is related to their electrochemical properties, which are influenced by their local protein environment. Quinones can be reduced in two successive reversible one-electron steps. The first step leads to an intermediate, a semiquinone (quinone anion radical); the second step, followed by protonation, leads to the fully reduced quinol (3,4). These properties make quinones ideally suited as electron and proton carriers in the bioenergetic processes of respiration and photosynthesis (5).

Two ubiquinones, Q_A and Q_B, are present in the reaction centers (RCs) of photosynthetic purple bacteria. Q_A accepts one-electron and is not protonated, whereas Q_B accepts, sequentially, two electrons. The second electron transfer is coupled with protonation leading to the formation of ubiquinol, which is weakly bound and diffuses out of the binding site to participate in the formation of the proton gradient required for ATP synthesis (5). Q_A and Q_B form hydrogen bonds to the RC protein. The bonds contribute to the binding and to the chemical properties and function of the quinones. It is, therefore, important to characterize the hydrogen bonds in detail.

Electron paramagnetic resonance (EPR) and electron nuclear double resonance (ENDOR) spectroscopies are ideally suited techniques to study the transient paramagnetic species involved in the primary events of photosynthesis, e.g., the ubiquinone anion radicals, $Q_A^{\cdot -}$ and $Q_B^{\cdot -}$. These studies provide information about the electronic and spatial structure of the transient radicals. In particular, $Q_A^{\cdot -}$ in the photosynthetic RC of *Rhodobacter sphaeroides* has been investigated extensively using EPR and ENDOR spectroscopies (6–12). These investigations showed that the ENDOR lines of $Q_A^{\cdot -}$ are due to three classes of protons: 1), protons associated with the protein in the vicinity of the binding site (matrix lines); 2), nonexchangeable protons on the quinone, e.g., methyl, methoxy, or methylene protons; and 3), exchangeable protons, the most important of which are the protons forming hydrogen bonds with the two carbonyl oxygens of the quinone. The ENDOR lines corresponding to the exchangeable protons were identified by comparing ENDOR spectra of RCs in H_2O and D_2O buffer (6).

The initial ENDOR results suggested that $Q_A^{\cdot -}$ is bound to the RC protein by two nonequivalent hydrogen bonds to the carbonyl oxygens of the quinone (7). Confirming evidence of two H-bonds was obtained by electron spin echo envelope modulation (ESEEM) (13–15). Additional, independent evidence of two nonequivalent hydrogen bonds was obtained by Paddock et al. (16), who showed that there are two different proton-deuterium exchange times associated with two distinct hydrogen bonded protons.

Based on the RC structure (17) the two hydrogen bonds were assigned to the imidazole nitrogen of His (M219) (N_δ-$H\cdots O_4$) and the NH group of Ala (M260) (N-$H\cdots O_1$) (see Fig. 1). However, there remained two problems: 1), in none of the previous experiments (6,7,16) could the ENDOR lines be assigned to protons associated with specific oxygens (i.e., O_1 or O_4, Fig. 1); and 2), there remained the puzzle why only three pairs of ^{1}H-ENDOR lines were observed instead of the expected four pairs (in randomly oriented molecules each

Submitted November 16, 2005, and accepted for publication January 18, 2006.

Address reprint requests to George Feher, E-mail: gfeher@ucsd.edu.

0006-3495/06/05/3356/07 $2.00

doi: 10.1529/biophysj.105.077883

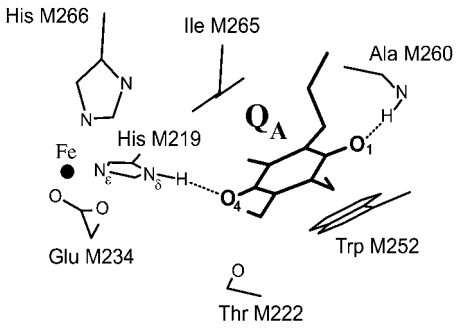

FIGURE 1 Structure in the vicinity of Q_A in the RC of *Rb. sphaeroides* (Brookhaven Protein Data Bank entry 1AIG (17)). The iron is ligated to four histidines (only two are shown) and one glutamate (bidentate ligand). The isoprenoid chain of the quinone is truncated for simplicity. The two carbonyl oxygens of the quinone, labeled 1 and 4, form H-bonds shown by dotted lines.

proton gives rise to two pairs of lines corresponding approximately to the parallel and perpendicular components of the axially symmetric hyperfine tensors). In this work we addressed both of these problems. We first determined the different $^1H \rightarrow {}^2H$ exchange times of the two hydrogen bonds by incubating protonated (or deuterated) RCs for different times in D_2O and monitoring the amplitudes of the ^1H-ENDOR lines. By using the results of these experiments we prepared RCs whose hydrogen bonds were preferentially deuterated (or protonated) at either O_1 or O_4. This enabled us to determine which set of ENDOR lines belong to a given oxygen. This solved the problem of the assignment of the observed three pairs of lines. Using the known structure of the RC (17) we postulated an assignment of each set of lines to a particular oxygen. A detailed simulation of the ENDOR spectra and the determination of the geometry of the H-bonds will be presented in a future article.

Hamiltonian of the spin system

In this study, we focus on the interaction between the magnetic moment of the unpaired electron of $Q_A^{\cdot -}$ and the magnetic moments of protons or deuterons that form hydrogen bonds to the quinone oxygens O_1 and O_4 (see Fig. 1). The observed ENDOR spectra were interpreted using a spin Hamiltonian, $\mathcal{H}$, containing the electron and nuclear Zeeman interactions with the applied magnetic field B_o, the hyperfine coupling (hfc) and the nuclear quadrupole coupling (nqc) terms (e.g., Weil et al. (18)):

$$\mathcal{H} = \beta_e \boldsymbol{S}\cdot\boldsymbol{g}\cdot\boldsymbol{B}_o - \beta_N g_N \mathrm{I}\cdot\boldsymbol{B}_o + h\boldsymbol{S}\cdot\boldsymbol{A}\cdot\boldsymbol{I} + h\boldsymbol{I}\cdot\boldsymbol{P}\cdot\boldsymbol{I}, \quad (1)$$

where $\boldsymbol{S}$ is the electron spin operator, $\boldsymbol{I}$ is the nuclear spin operator of protons or deuterons in H-bonds to the carbonyl oxygens; $\boldsymbol{A}$ and $\boldsymbol{P}$ are the hfc and nqc tensors in frequency units, g is the electronic g-tensor, h is Planck's constant, g_N is the g-factor of the corresponding magnetic nucleus (proton or deuteron), and β_e and β_N are the electron and nuclear magnetons, respectively.

The first term in Eq. 1 represents the electronic Zeeman term that gives rise to the observed EPR spectrum. The other three terms represent nuclear interactions that give rise to the ENDOR spectra. These can be calculated to first order from Eq. 1 using an expansion in powers of the ratio $hA/(g\beta_e B_o)$ (18,19). At the microwave frequency of 35 GHz used in this work, second order terms are small and can be neglected. Furthermore, at 35 GHz the ENDOR free frequency of protons (or deuterons) is much larger than its respective hfc interaction, i.e., $g_N\beta_N B_o/h \gg A/2$. Thus, the resonance frequency of the ENDOR transition $M_\gamma \leftrightarrow M_\gamma - 1$ is given to first order for a given direction of the magnetic field by (18,19):

$$\nu_{ENDOR} = g_N\beta_N B_o/h - AM_S - \frac{3}{2}P(2M_\gamma - 1), \quad (2)$$

where M_S is the magnetic quantum number of the electron ($\pm$½) and M_γ the magnetic quantum number corresponding to the lower energy levels of the nucleus, i.e., +½ for protons and +1, 0 for deuterons.

For protons $M_\gamma = +½$ making the term containing the nuclear quadrupole interaction P zero. Thus, for a given magnetic field direction with respect to the molecular axes, one expects two ENDOR lines separated by the hfc A centered around the proton Larmor frequency $g_N\beta_N B_o/h$. For deuterons $M_\gamma = +1, 0$ and each line is additionally split by $3P$. In a sample having randomly oriented molecules, the anisotropies of A and P smear out the spectrum and sharp lines are observed only at the extrema (e.g., approximately at $A_{//}$ and $A_\perp$).

At 35 GHz (Q-band) the anisotropies of the electronic g-value gives rise to a spectrum shown in Fig. 2. At the positions labeled g_x, g_y, and g_z, the majority of the molecules contributing to the spectrum have their molecular axes along the principal directions x, y, and z. However, it should be noted that at each position there is a significant admixture of molecules having different directions. Thus, only a partial magnetic field selection of orientations is obtained.

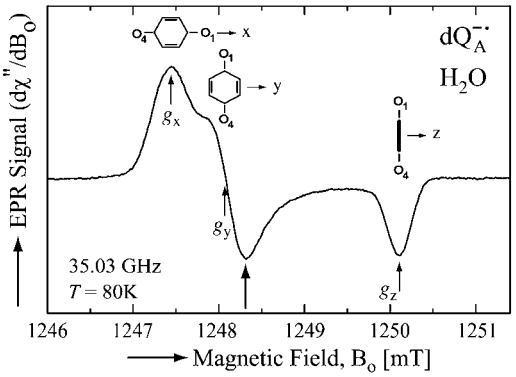

FIGURE 2 EPR powder spectrum of $dQ_A^{\cdot -}$ in H_2O. Insets show the quinone orientations with respect to the magnetic field corresponding to g_x, g_y, and g_z. Experimental conditions: T = 80 K, MW frequency = 35.03 GHz, MW power = 1×10^{-7} W, field modulation = 0.15 mT peak-to-peak at 270 Hz, average of 9 scans, 20 s per scan.

At Q-band the magnetic field B_o is ~1.25 T and the ENDOR lines for protons and deuterons are observed in different frequency ranges, ~53 MHz for ^{1}H and ~8 MHz for ^{2}H. This enabled us to separate the signals due to protons in H-bonds from those in the quinone ring by using samples of deuterated RCs in H_2O buffer. To observe deuterons in H-bonds we used samples of protonated RCs in D_2O buffer.

MATERIALS AND METHODS

Preparation of reaction centers

RCs from *Rb. sphaeroides* R-26 were isolated and purified following the procedures of Isaacson et al. (9). The paramagnetic nonheme Fe^{2+} was chemically removed and replaced with diamagnetic Zn^{2+} to reduce the EPR line width of the semiquinone, following the procedure of Utschig et al. (20). The ratio of Zn/RC was determined by atomic absorption spectroscopy and Q-band EPR spectroscopy to be ≥0.90.

Deuteration of reaction centers

Fully deuterated RCs were obtained by growing *Rb. sphaeroides* R-26 bacteria in a D_2O-based modified Hutner's medium using perdeuterated succinic acid (98% D, Aldrich, Milwaukee, WI) as the sole carbon source as described previously by van der Est et al. (21).

Proton-deuterium exchange

We used two sets of samples in which protons were exchanged with deuterons—one for the determination of the exchange times and the other for obtaining detailed ENDOR spectra, which required a higher signal/noise ratio, i.e., a higher RC concentration.

For the determination of the exchange times, fully protonated and fully deuterated RCs were purified and concentrated to an optical absorbance of $A_{800}^{1cm} \approx 200$. The RC samples were diluted into D_2O buffer for different lengths of time, at the end of which Q_A^- was generated photochemically (see next section) and frozen by immersing the sample in liquid nitrogen. We used a fivefold dilution for deuterated RCs and a fourfold dilution for protonated RCs. The final optical absorbance A_{800}^{1cm} was ~40 and ~50, respectively.

To obtain ENDOR spectra in which one of the H-bonds was preferentially deuterated, we prepared the following high concentration ($A_{800}^{1cm} \approx 200$) samples:

1. Deuterated RCs in H_2O buffer incubated for 27 min in D_2O buffer (10-fold dilution).
2. Protonated RCs in H_2O buffer incubated for 50 min in D_2O buffer (fivefold dilution).
3. Protonated RCs in D_2O buffer incubated for 190 min in H_2O buffer (300-fold dilution).

The incubation times (see section on ENDOR results) and dilutions were chosen to maximize the preferential deuteration of one of the H-bonds to Q_A. After dilution the samples were concentrated by centrifuging in a Millipore (5–50k) filter to an optical absorbance $A_{800}^{1cm} \approx 200$. At the end of the incubation Q_A^- was generated chemically (see next section) and the sample frozen by immersing it in liquid nitrogen.

Generation of semiquinone radical anion

We used two methods to generate Q_A^-: 1), for low concentration samples ($A_{800}^{1cm} \leq 50$) we illuminated the RCs with a single, saturating laser flash (Lumen-X DL2100C, $\lambda = 590$ nm) in the presence of excess cyt c_2 to reduce the donor, D^+, and stigmatellin to inhibit electron transfer to Q_B (photochemical method). After the laser flash the sample was plunged into liquid nitrogen. 2), For high concentration samples ($A_{800}^{1cm} \geq 200$), we used $Na_2S_2O_4$ to reduce Q_A before freezing (chemical method) (6). The quartz sample tubes were type 705PQ (Wilmad, Buena, NJ) (OD 3 mm, ID 2 mm).

Nomenclature

Since we used several combinations of protonated and deuterated RCs and buffer, we define the following notation: *a*), ($pQ_A^{\cdot -}$) for Q_A^- in fully protonated RCs and ($dQ_A^{\cdot -}$) for Q_A^- in fully deuterated RCs; *b*), (H_2O) for fully protonated buffer and (D_2O) for fully deuterated buffer; and *c*), ($H_2O \xrightarrow{time} D_2O$) for RCs prepared in H_2O and incubated later in D_2O for a specific time (in minutes) and ($D_2O \xrightarrow{time} H_2O$) for the reverse.

EPR instrumentation

EPR and ENDOR measurements were performed at 35 GHz and 80 K. The spectrometer is a home-built superheterodyne-type instrument with a Varian klystron, a cylindrical TE_{011} brass cavity, and an immersion dewar system for temperature control. The cavity and coupler is similar to one described by Jaworski et al. (22). A Li:LiF sample was used as a primary g-value standard ($g = 2.00229$) (23), and P-doped Si as a secondary standard ($g = 1.99891$ at 80 K) (24,25). The P-Si marker was permanently attached to the bottom wall of the cavity. ENDOR experiments were performed with the EPR spectra 50% saturated. ENDOR spectra were recorded at the magnetic field positions as indicated in the corresponding traces, using frequency modulation (FM) of ±140 kHz for protons and ±30 kHz for deuterons, at FM rates as indicated in the figure captions. The output of the RF amplifier (ENI 3100L) feeding the ENDOR coils was 50 W for protons and 25 W for deuterons. To improve the signal/noise ratio of the ENDOR signal, many traces were averaged for up to 3 h for protons and 42 h for deuterons.

EXPERIMENTAL RESULTS AND DISCUSSION

EPR results

The Q-band EPR spectrum from $dQ_A^{\cdot -}$ in protonated buffer (H_2O), at $T = 80$ K, is shown in Fig. 2. The broadening of the spectrum is mainly due to protons in solution (exchangeable protons), including the H-bonds to the carbonyl oxygens. Exchanging H_2O with D_2O, decreases the broadening (data not shown).

ENDOR results

^{1}H ENDOR spectrum corresponding to the H-bonds

Fig. 3 shows the Q-band ^{1}H ENDOR spectrum at $T = 80$ K of $dQ_A^{\cdot -}$ in H_2O (chemically reduced), arising from ^{1}H-bonds and from protons in the solvent. The spectrum was recorded at the magnetic field corresponding to g_y (see Fig. 2). The splittings of the ^{1}H-ENDOR peaks associated with the H-bonds are A_1 (4.82 MHz), A_2 (6.43 MHz), and A_3 (9.07 MHz). Similar splittings were previously observed at X-band by comparing ENDOR spectra of Q_A^- in H_2O and D_2O (6,12).

As described in the Spin Hamiltonian section, the single-crystal ^{1}H ENDOR spectrum corresponding to a proton

contains two lines (see Eq. 2). However, at the magnetic field position corresponding to g_y, the spectrum corresponds to a ''two-dimensional'' powder-type spectrum, with weighted contributions mainly from all in-plane directions. Therefore, a powder spectrum is expected for each H-bond tensor with two sharp features, corresponding approximately to the parallel ($A_{//}$) and the perpendicular ($A_\perp$) components of an axially symmetric hfc tensor (7,26–28), i.e., each proton should give rise to two pairs of lines. For benzoquinone anion radicals in solution, the ENDOR experiments showed that the H-bond hfc tensor is approximately axially symmetric. This is typical for a proton in a normal H-bond. Deviations are expected only for very short H-bonds as described in (29). Since in reaction centers there are two nonequivalent H-bonds to $Q_A^{\cdot-}$ (12–16), in principle four pairs of ^{1}H ENDOR lines should be observed in the spectrum. However, the experiment shows only three pairs, despite a thorough search for a fourth set of lines. This problem is discussed in a subsequent section.

There are two problems to be solved in the identification of the ENDOR lines associated with the hydrogen-bonded protons: 1), which pair of lines belong to the same proton; and 2), with which oxygen (O_1 or O_4) is a particular set of ENDOR lines associated.

To answer the first question we make use of the selective deuteration of the oxygens as discussed in the next section.

Determination of the $^1H \rightarrow {}^2H$ exchange times of the two protons H-bonded to Q_A

To preferentially deuterate one of the H-bonds to Q_A, it is necessary to determine their respective $^1H \rightarrow {}^2H$ exchange times. We used ENDOR to measure the $^1H \rightarrow {}^2H$ exchange times of the two protons H-bonded to Q_A, in fully deuterated RCs and in fully protonated RCs (R-26). In the fully deuterated RCs in H_2O we measured the amplitudes of the ^{1}H-ENDOR lines L_1 and L_2 corresponding to the two protons (Fig. 3) at different times of incubation in D_2O. The incubation time started with a fivefold dilution of the H_2O sample in D_2O. The semiquinone $Q_A^{\cdot-}$ was produced photochemically (see Materials and Methods) at the end of the incubation period.

In view of the fivefold dilution of the sample, 20% of the bonds remain protonated and only 80% are subject to exchange with deuterium. Thus, the normalized ratio of amplitudes of L_1 to L_2 is given by:

$$\frac{(L_1/L_1^0)}{(L_2/L_2^0)} = \frac{[0.2 + 0.8\exp(-t/\tau_1)]}{[0.2 + 0.8\exp(-t/\tau_2)]}, \qquad (3)$$

where L_1^0 and L_2^0 are the respective initial intensities and τ_1 and τ_2 are the respective $^1H \rightarrow {}^2H$ exchange times for the two protons. For protonated RCs, the H_2O samples were diluted fourfold in D_2O.

Fig. 4 shows the observed time dependence of the normalized intensity ratio of the L_1 and L_2 lines for fully deuterated and fully protonated RCs. The $^1H \rightarrow {}^2H$ exchange times were determined by fitting the experimental data with Eq. 3, with τ_1 and τ_2 as adjustable parameters. The resultant values of τ_1 and τ_2 are shown in the inserts of Fig. 4.

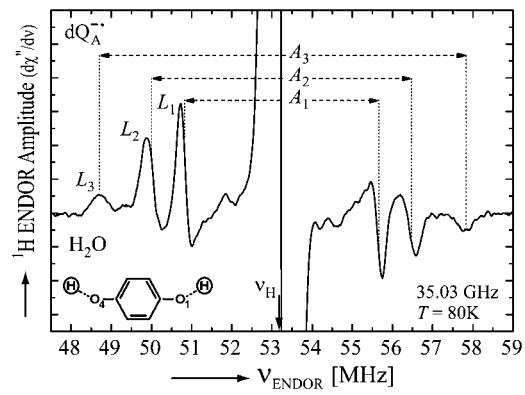

FIGURE 3 ^{1}H ENDOR spectrum of $dQ_A^{\cdot-}$ in H_2O. The spectrum was taken at the field position corresponding to $g_y = 2.0053$ (see Fig. 2). The intensities of the transitions are denoted by L_1, L_2, L_3, and the hyperfine coupling constants by A_1, A_2, A_3. Experimental conditions: $T = 80$ K, MW frequency = 35.03 GHz, MW power = 3×10^{-6} W; FM = ±140 kHz at a rate of 947 Hz. Number of scans: 500. Scan time: 4 s.

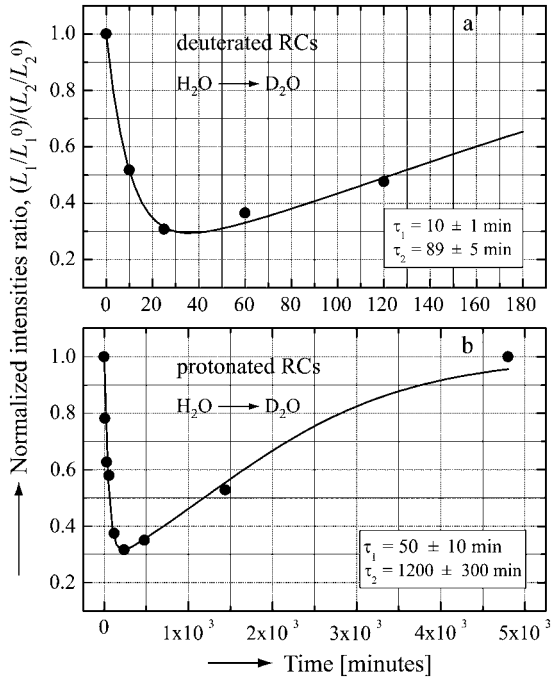

FIGURE 4 The normalized intensities ratios $(L_1/L_1^0)/(L_2/L_2^0)$ for the low frequency ^{1}H-ENDOR lines (see Fig. 3), as a function of the incubation time in D_2O for deuterated RCs (*a*) and for protonated RCs (*b*). The $^1H \rightarrow {}^2H$ exchange times were obtained by fitting the experimental data (*dots*) with Eq. 3 (*solid lines*). The values of the exchange times τ_1 and τ_2 are shown in the inserts. Experimental conditions: Microwave frequency 35 GHz, $T = 80$ K, B_o at position corresponding to g_y (see Fig. 2). Optical absorbance of sample $A_{800}^{1cm} = 40$ (*a*) and 50 (*b*).

The different exchange times observed for protonated and deuterated RCs is believed to reflect the structural changes in the RCs when the bacteria are grown in a fully deuterated medium. The shorter exchange times in deuterated RCs suggest a less compact structure, in which the quinone oxygens are more accessible to the solvent. Paddock et al. (16), who measured the exchange times in protonated RCs of the HC (M266) mutant, found an order of magnitude different times than in the wild-type, suggesting again a structural change. Thus, the exchange times are very sensitive to the details of the structure and may provide a useful probe in investigating structural changes.

Assignment of pairs of lines belonging to the same proton

To solve this problem we used the differential exchange of one proton with respect to the other as discussed in the previous section. The lines associated with a particular proton should show the same reduction in amplitude when the proton is exchanged with deuterons. Fig. 5 shows the low frequency part of the ^{1}H-ENDOR spectrum of $dQ_A^{\cdot-}$ in H_2O (*top*) and after 27 min of exchanges in D_2O (*bottom*), both samples were produced chemically. Deuterated RCs were used to eliminate ENDOR signals from protons of the protein. Using the exchange times for the two protons of 10 min and 89 min, respectively (see Fig. 4 *a*), we predict that one proton should be ~80% exchanged and the other ~20%. The reduction in amplitudes of L_1 and L_2 correspond roughly to these values. Thus, the peaks L_1 and L_2 are associated with two different protons, as had been postulated previously (7,16).

We now turn to the assignment of the line corresponding to the largest hyperfine coupling (see left of Fig. 5). Does it represent the partner to L_1 or L_2? We shall show that this line is an overlap of two lines, one being a partner to L_1 and the other to L_2. The proof is as follows: The exchange reduced the amplitude of L_1 8.1-fold (130/16; see Table 1). If the peak were only the partner of L_1 we would expect it to decrease to 1.1 units. The observed peak is 4 units, i.e., significantly larger, showing that a considerable part of it is associated with another line, L_4, the partner to L_2, thus confirming the overlap. The effect is best observed for a magnetic field position slightly off g_y (at $B_o = 1248.3$ mT; see Fig. 2).

Additional evidence for the overlap is provided by the ^{2}H-ENDOR spectra of protonated RCs in D_2O shown in Fig. 6 (high concentration samples; see Materials and Methods). Each ^{2}H-ENDOR line is split into a doublet by the nuclear quadrupole interaction, $3P$ (Eq. 2). The center of each doublet (*solid arrows* in Fig. 6) corresponds to the hfc (18). The top trace shows the low frequency ^{2}H-ENDOR spectrum after incubating the RC for 50 min in D_2O. In these experiments protonated RCs were used to eliminate signals from the protein. With the exchange times of 50 min and 1200 min (Fig. 4 *b*), we expect one oxygen (O_a) to be ~50% deuterated, whereas the other (O_b) only ~3% (see Eq. 3 and

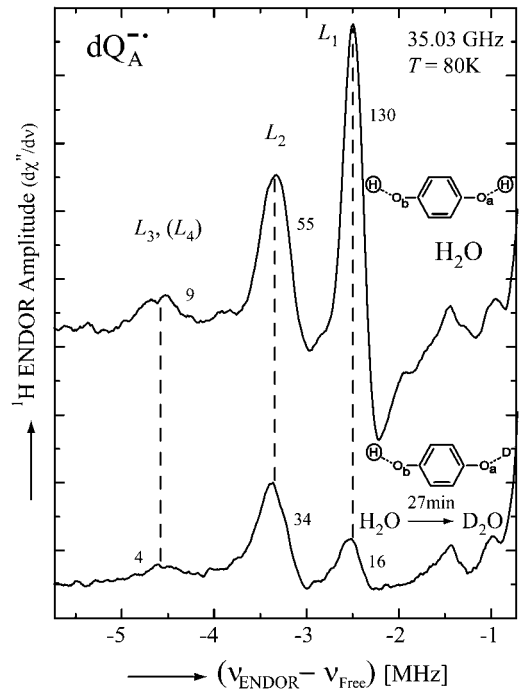

FIGURE 5 Low-frequency part of the ^{1}H ENDOR spectra of $dQ_A^{\cdot-}$ in H_2O (*upper spectrum*) and in $H_2O \xrightarrow{27\,min} D_2O$ (*lower spectrum*), at 35 GHz, taken at a magnetic field of 1248.3 mT (see *arrow* in Fig. 2). The H-bond ENDOR lines are labeled L_1, L_2, L_3, and L_4 in the upper spectrum. Numbers next to each line refer to their amplitudes (in arbitrary units) (see Table 1). Experimental conditions: $T = 80$ K, MW power = $\sim 3 \times 10^{-6}$ W, FM = $\pm$140 kHz at a rate of 950 Hz. Number of scans: 500 (*upper spectrum*) and 2860 (*lower spectrum*). Scan time: 4 s.

inset in Fig. 6, *top*). Thus, the spectrum is essentially due to deuterons on O_a. In the lower trace the deuterons were exchanged with protons giving rise to an ^{2}H-ENDOR spectrum associated with deuterons on O_b (see *inset* in Fig. 6, *bottom*). Comparing the two spectra we see that the low frequency line (at −0.8 MHz) of P_3 is shifted by ~30 kHz from that of P_4 showing that the two lines belong to different D-bonds. The shift between the two lines is smaller than the line width which explains why the two lines are not resolved when both oxygens are protonated (or deuterated). These results clearly show that the line at −0.8 MHz is associated with deuterons on both O_a and O_b.

Assignment of the ENDOR lines of the hydrogen bonds to a particular (O_1 or O_4) oxygen

In the previous section we refer to O_a and O_b as being associated with a given set of ENDOR lines. Our goal is to

TABLE 1 Amplitudes of the ^{1}H ENDOR lines (in arbitrary units) corresponding to the protons H-bonded to $dQ_A^{\cdot-}$ in H_2O (before exchange) and in $H_2O \xrightarrow{27\,min} D_2O$ (after exchange) (see Fig. 5)

	$L_3 + L_4$	L_2	L_1
Before exchange	9	55	130
After exchange	4	34	16

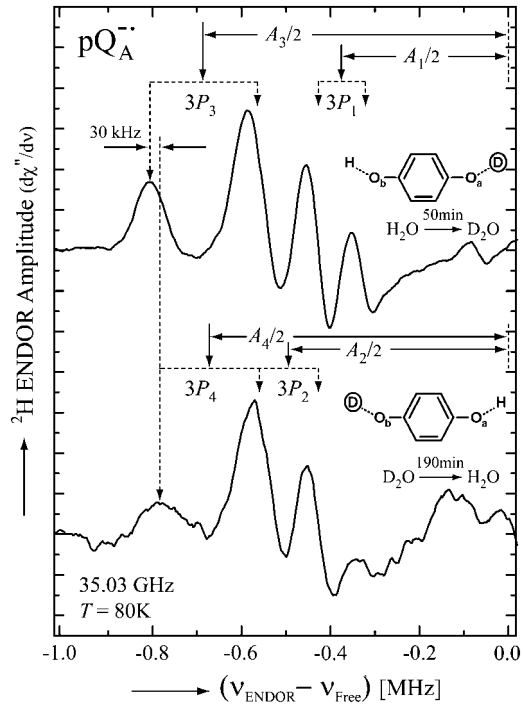

FIGURE 6 Low-frequency part of the ^{2}H ENDOR spectra of $pQ_A^{\cdot -}$ in $H_2O \xrightarrow{50\,min} D_2O$ (*upper spectrum*) and in $D_2O \xrightarrow{190\,min} H_2O$ (*lower spectrum*), at 35 GHz, taken along the magnetic field position corresponding to g_y (see Fig. 2). The position of the hfc tensor components (A_1, A_2, A_3, and A_4) are indicated by solid arrows, whereas the nqc splittings ($3P_1$, $3P_2$, $3P_3$, and $3P_4$) are indicated by dotted arrows. Inserts show the preferential deuteration of the carbonyl oxygens. Experimental conditions: $T = 80$ K, MW power = $\sim 5 \times 10^{-6}$ W, FM = $\pm$30 kHz at a rate of 985 Hz. Number of scans: 8000 (*upper spectrum*) and 37,000 (*lower spectrum*). Scan time: 4 s.

relate these results to the specific oxygen, O_1 and O_4 of the quinones (see Fig. 1). This, unfortunately, cannot be accomplished from the ENDOR experiments discussed above. We know, however, from the x-ray structure (17) that Ala (M260), i.e., O_1, is closer to the surface of the RC and is, therefore, expected to exchange its proton faster than the buried His (M219), i.e., O_4. Furthermore, EPR (8,10,30) and FTIR (31,32) experiments on ^{13}C substituted quinones showed that the hydrogen bond to O_1 is weaker than to O_4 (reviewed in Lubitz and Feher (12). We, therefore, postulate that the ENDOR line L_1 and L_3 (Fig. 5) are associated with O_1 and L_2 and L_4 with O_4. This assignment will be further validated in a subsequent publication.

CONCLUSION

We have identified the ^{1}H and ^{2}H-ENDOR lines with the hfcs of the specific protons hydrogen bonded to the two carbonyl oxygens on $Q_A^{\cdot -}$ in reaction centers of *Rb. sphaeroides*. In a forthcoming study, these assignments will be used to determine the exact geometries of the hydrogen bonds.

We thank M. Paddock (University of California, San Diego) for providing data on the ^{1}H/^{2}H exchange times in protonated Zn-RCs (Fig. 4 *b*) and for helpful discussions.

This work was supported by National Science Foundation MCB 99/82186 and National Institutes of Health GM13191 and by Max Planck Society, and Fonds der Chemischen Industrie (to W.L.).

REFERENCES

1. Lenaz, G., editor. 1985. Coenzyme *Q*: Biochemistry, Bioenergetics and Clinical Applications of Ubiquinone. John Wiley & Sons, Chichester; New York.
2. Trumpower, B. L. 1982. Function of Quinones in Energy Conserving Systems. Academic Press, New York
3. Chambers, J. Q. 1988. Electrochemistry of quinones. *In* The Chemistry of Quinonoid Compounds. S. Patai and Z. Rappoport, editors. John Wiley & Sons, Chichester; New York. 719–757.
4. Morrison, L. E., J. E. Schelhorn, T. M. Cotton, C. L. Bering, and P. A. Loach. 1982. Electrochemical and spectral properties of ubiquinone and synthetic analogs: Relevance to bacterial photosynthesis. In Function of quinones in energy conserving systems. B. L. Trumpower, editor. Academic Press, New York. 35–58.
5. Cramer, W. A., and D. B. Knaff. 1990. The quinone connection. *In* EnergyTransduction in Biological Membranes. C. R. Cantor, editor. Springer-Verlag, New York. 193–238.
6. Lubitz, W., E. C. Abresch, R. J. Debus, R. A. Isaacson, M. Y. Okamura, and G. Feher. 1985. Electron nuclear double resonance of semiquinones in reaction centers of *Rhodopseudomonas sphaeroides*. *Biochim. Biophys. Acta.* 808:464–469.
7. Feher, G., R. A. Isaacson, M. Y. Okamura, and W. Lubitz. 1985. ENDOR of semiquinones in RCs from *Rhodopseudomonas sphaeroides*. *In* Antennas and Reaction Centers of Photosynthetic Bacteria-Structure, Interactions and Dynamics. M. E. Michel-Beyerle, editor. Springer-Verlag, Berlin. 174–189.
8. van den Brink, J. S., A. P. Spoyalov, P. Gast, W. B. S. van Liemt, J. Raap, J. Lugtenburg, and A. J. Hoff. 1994. Asymmetric binding of the primary acceptor quinone in reaction centers of the photosynthetic bacterium *Rhodobacter sphaeroides* R26, probed with *Q*-Band (35 GHz) EPR spectroscopy. *FEBS Lett.* 353:273–276.
9. Isaacson, R. A., F. Lendzian, E. C. Abresch, W. Lubitz, and G. Feher. 1995. Electronic structure of $Q_A^{\cdot -}$ in reaction centers from *Rhodobacter sphaeroides*. 1. Electron paramagnetic resonance in single crystals. *Biophys. J.* 69:311–322.
10. Isaacson, R., E. C. Abresch, F. Lendzian, C. Boullais, M. Paddock, C. Mioskowski, W. Lubitz, and G. Feher. 1996. Asymmetry of the binding sites of $Q_A^{\cdot -}$ and $Q_B^{\cdot -}$ in reaction centers of *Rb. sphaeroides* probed by *Q*-band EPR with ^{13}C-labeled quinones. *In* The Reaction Center of Photosynthetic Bacteria: Structure and Dynamics. M. E. Michel-Beyerle, editor. Springer-Verlag, Berlin. 353–367.
11. Rohrer, M., F. MacMillan, T. F. Prisner, A. T. Gardiner, K. Mobius, and W. Lubitz. 1998. Pulsed ENDOR at 95 GHz on the primary acceptor ubisemiquinone $Q_A^{\cdot -}$ in photosynthetic bacterial reaction centers and related model systems. *J. Phys. Chem. B.* 102:4648–4657.
12. Lubitz, W., and G. Feher. 1999. The primary and secondary accepters in bacterial photosynthesis III. Characterization of the quinone radicals $Q_A^{\cdot -}$ and $Q_B^{\cdot -}$ by EPR and ENDOR. *Appl. Magn. Reson.* 17:1–48.
13. Bosch, M. K., P. Gast, A. J. Hoff, A. P. Spoyalov, and Y. D. Tsvetkov. 1995. The primary acceptor quinone Q_A in reaction centers of *Rhodobacter-sphaeroides* R26 is hydrogen-bonded to the $N^{\delta(1)}$-H of His M219. An electron-spin echo study of $Q_A^{\cdot -}$. *Chem. Phys. Lett.* 239:306–312.
14. Lendzian, F., J. Rautter, H. Kass, A. Gardiner, and W. Lubitz. 1996. ENDOR and pulsed EPR studies of photosynthetic reaction centers: protein-cofactor interactions. *Ber. Bunsenges. Phys. Chem.* 100:2036–2040.

15. Spoyalov, A. P., R. J. Hulsebosch, S. Shochat, P. Gast, and A. J. Hoff. 1996. Evidence that Ala M260 is hydrogen-bonded to the reduced primary acceptor quinone Q_A^- in reaction centers of *Rb. sphaeroides*. *Chem. Phys. Lett.* 263:715–720.

16. Paddock, M. L., E. C. Abresch, R. A. Isaacson, W. Lubitz, M. Y. Okamura, and G. Feher. 1999. Identification of hydrogen bonds to Q_A^- in RCs of *Rb. sphaeroides* by ENDOR spectroscopy. *Biophys. J.* 76:A141–A141.

17. Stowell, M. H. B., T. M. McPhillips, D. C. Rees, S. M. Soltis, E. Abresch, and G. Feher. 1997. Light-induced structural changes in photosynthetic reaction center: implications for mechanism of electron-proton transfer. *Science*. 276:812–816.

18. Weil, J. A., J. R. Bolton, and J. E. Wertz. 1994. Electron Paramagnetic Resonance. Elementary Theory and Practical Applications. Wiley, New York.

19. Weil, J. A. 1975. Comments on second-order spin Hamiltonian energies. *J. Magn. Reson.* 18:113–116.

20. Utschig, L. M., S. R. Greenfield, J. Tang, P. D. Laible, and M. C. Thurnauer. 1997. Influence of iron-removal procedures on sequential electron transfer in photosynthetic bacterial reaction centers studied by transient EPR spectroscopy. *Biochemistry*. 36:8548–8558.

21. van der Est, A., R. Bittl, E. C. Abresch, W. Lubitz, and D. Stehlik. 1993. Transient EPR spectroscopy of perdeuterated Zn-substituted reaction centers of *Rhodobacter sphaeroides* R-26. *Chem. Phys. Lett.* 212:561–568.

22. Jaworski, M., A. Sienkiewicz, and C. P. Scholes. 1997. Double-stacked dielectric resonator for sensitive EPR measurements. *J. Magn. Reson.* 124:87–96.

23. Stesmans, A., and G. Vangorp. 1989. Novel method for accurate *g*-measurements in electron-spin resonance. *Rev. Sci. Instrum.* 60:2949–2952.

24. Feher, G., and E. Gere. 1959. Electron spin resonance experiments on donors in silicon. II. Electron spin relaxation effects. *Phys. Rev.* 114:1245–1256.

25. Stesmans, A., and G. Devos. 1986. Electron-spin-resonance observation of temperature dependent *g* shifts in submetallic P doped Si at low temperatures. *Phys. Rev. B*. 34:6499–6502.

26. O'Malley, P. J., and G. T. Babcock. 1986. Powder ENDOR spectra of para-benzoquinone anion radical principal hyperfine tensor components for ring protons and for hydrogen-bonded protons. *J. Am. Chem. Soc.* 108:3995–4001.

27. MacMillan, F., F. Lendzian, and W. Lubitz. 1995. EPR and ENDOR characterization of semiquinone anion radicals related to photosynthesis. *Magn. Reson. Chem.* 33:S81–S93.

28. Flores, M., R. A. Isaacson, R. Calvo, G. Feher, and W. Lubitz. 2003. Probing hydrogen bonding to quinone anion radicals by ^1H and ^2H ENDOR spectroscopy at 35 GHz. *Chem. Phys.* 294:401–413.

29. Sinnecker, S., E. Reijerse, F. Neese, and W. Lubitz. 2004. Hydrogen bond geometries from electron paramagnetic resonance and electron-nuclear double resonance parameters: density functional study of quinone radical anion-solvent interactions. *J. Am. Chem. Soc.* 126: 3280–3290.

30. Hoff, A. J., T. N. Kropacheva, R. I. Samoilova, N. P. Gritzan, J. Raap, J. S. van den Brink, P. Gast, and J. Lugtenburg. 1996. Site-directed isotope labelling as a tool in spectroscopy of photosynthetic preparations. Investigations on quinone binding in bacterial reaction centers. *In* The Reaction Center of Photosynthetic Bacteria: Structure and Dynamics. M. E. Michel-Beyerle, editor. Springer-Verlag, Berlin. 405–420.

31. Breton, J., C. Boullais, J. R. Burie, E. Nabedryk, and C. Mioskowski. 1994. Binding sites of quinones in photosynthetic bacterial reaction centers investigated by light-induced FTIR difference spectroscopy: assignment of the interactions of each carbonyl of Q_A in *Rhodobacter sphaeroide*s using site-specific ^{13}C-labeled ubiquinone. *Biochemistry*. 33:14378–14386.

32. Brudler, R., H. J. M. de Groot, W. B. S. van Liemt, W. F. Steggerda, R. Esmeijer, P. Gast, A. J. Hoff, J. Lugtenburg, and K. Gerwert. 1994. Asymmetric binding of the 1- and 4-C=O groups of Q_A in *Rhodobacter sphaeroides* R26 reaction centres monitored by Fourier transform infra-red spectroscopy using site-specific isotopically labelled ubiquinone-10. *EMBO J.* 13:5523–5530.